

1 **Changing seasonality of moderate and extreme precipitation events in the Alps**

2 Stefan Brönnimann^{1,2}, Jan Rajczak³, Erich M. Fischer³, Christoph C. Raible^{1,4}, Marco Rohrer^{1,2},
3 Christoph Schär³

4

5 ¹ Oeschger Centre for Climate Change Research, University of Bern, Switzerland

6 ² Institute of Geography, University of Bern, Switzerland

7 ³ Institute for Atmospheric and Climate Science, ETH Zurich, Switzerland

8 ⁴ Climate and Environmental Physics, Physics Institute, University of Bern, Switzerland

9

10 **Abstract.** The intensity of precipitation events is expected to increase in the future. The rate of
11 increase depends on the strength or rarity of the events; very strong and rare events tend to follow the
12 Clausius-Clapeyron relation, whereas weaker events or precipitation averages increase at a smaller
13 rate than expected from the Clausius-Clapeyron relation. An often overlooked aspect is seasonal
14 occurrence of such events, which might change in the future. To address the impact of seasonality, we
15 use a large ensemble of regional and global climate model simulations, comprising tens of thousands
16 of model years of daily temperature and precipitation for the past, present and future. In order to make
17 the data comparable, they are quantile-mapped to observation-based time series representative of the
18 Aare catchment in Switzerland. Model simulations show no increase in annual maximum 1-day
19 precipitation events (Rx1day) over the last 400 yrs and an increase of 10-20% until the end of the
20 century for a strong (RCP8.5) forcing scenario. This fits with a Clausius-Clapeyron scaling of
21 temperature at the event day, which increases less than annual mean temperature. An important reason
22 for this is a shift in seasonality. Rx1day events become less frequent in late summer and more frequent
23 in early summer and early fall, when it is cooler. The seasonality shift is shown to be related to
24 summer drying. Models with decreasing annual mean or summer mean precipitation show this
25 behaviour more strongly. The highest Rx1day per decade, in contrast, shows no change in seasonality
26 in the future. This discrepancy implies that decadal-scale extremes are thermodynamically limited;
27 conditions conducive to strong events still occur during the hottest time of the year on a decadal scale.
28 In contrast, Rx1day events are also limited by other factors. Conducive conditions are not reached
29 every summer in the present, and even less so in the future. Results suggest that changes in the
30 seasonal cycle need to be accounted for when preparing for moderately extreme precipitation events
31 and assessing their socio-economic impacts.

32 1. Introduction

33 Heavy precipitation extremes in the Alps may trigger flood events or landslides that lead to loss of
34 lives, cause large monetary losses and threaten important infrastructure. While the most extreme
35 events have the highest socio-economic impact, even moderate extreme events such as the annual
36 maximum rainfall (Rx1day) or events with a 10-yr return period may be relevant for climate change
37 adaptation. Even for these events, the observation records at a single location may not be long enough
38 to capture trends. Still, aggregating weather station records from Switzerland, Scherrer et al. (2016)
39 found an increase in intensity as measured by the magnitude of the annual maximum 1-day
40 precipitation extreme (Rx1day) or exceedances of the 99th percentile.

41 Heavy precipitation requires moisture convergence and convection or synoptic-scale uplift. With
42 increasing temperatures, saturation specific humidity increases and as a consequence an increased
43 precipitation intensity is expected. At the global scale, precipitation is limited by radiation that has to
44 balance the latent heat release (e.g. Allen and Ingram 2002). For extreme precipitation events,
45 however, Scherrer et al. (2016) found that the increase closely follows a Clausius-Clapeyron scaling of
46 the annual mean temperature trend. Fischer and Knutti (2016) also found a close to Clausius-
47 Clapeyron scaling to regional temperature changes both in global models and observations. However,
48 the scaling may not hold exactly for various reasons (Pendergrass 2018).

49 Firstly, global models do not resolve changes in convection (Prein et al., 2015; Zhang et al., 2017),
50 which is important for the case of Alpine precipitation (Giorgi et al., 2016). For instance, trends in
51 Alpine precipitation are different during summer in convection-resolving regional models (Ban et al.,
52 2014). Secondly, the scaling of extreme precipitation with temperatures at day-to-day time scales
53 cannot generally be extrapolated to the future based on annual or seasonal mean temperatures (e.g.,
54 Ban et al. 2015; Schär et al 2016; Zhang et al. 2017). One possible cause for a discrepancy between
55 scaling at day-to-day time scales and at time scales of long-term warming is a potential change in
56 seasonality. Pfahl et al. (2017) in an analysis of CMIP5 data (Taylor et al., 2012), found a shift in the
57 future Rx1day towards smaller saturation specific humidity over most of the northern extratropical
58 land areas (their Fig. S6), indicative of lower temperatures and thus a shift towards the colder seasons.
59 Recently, Messmer et al. (submitted) focused on one dynamical feature, which is responsible for
60 extreme precipitation events in the Alps, the so-called Vb cyclone (van Bebber, 1898; Messmer et al.,
61 2015). They found in dynamically downscaled scenario simulations (RCP 8.5) that the occurrence of
62 extreme Vb cyclones is shifted from the midsummer to May and September in the future.

63 In this paper we focus on seasonality changes of heavy precipitation events (Rx1day) in the Alps using
64 a comprehensive set of global and regional model simulations comprising tens of thousands of years
65 of daily temperature and precipitation quantile mapped to observations representative of a large
66 catchment in Switzerland. Based on this comprehensive data set, we analyse (1) trends in Rx1day and

67 their relation to temperature trends, (2) the effect of changes in the seasonal cycle of temperature on
68 Rx1day events and (3) the effect of changes in the seasonal frequency of occurrence of Rx1day.

69 The paper is organised as follows. Section 2 gives a brief overview of the data and the quantile
70 mapping approach (Rajczak et al., 2018) and outlines the analyses performed. Section 3 presents the
71 results for Rx1day. A discussion in terms of underlying mechanisms and differences between models
72 and model set-ups follows in Section 4. Conclusions are drawn in Section 5.

73

74 **2. Data and Methods**

75 The study focuses on the Aare river catchment in Switzerland, an area of approximately 17 000 km²
76 (see Fig. 1). Heavy precipitation events in this catchment can cause major floods of the lower Aare
77 river and the Rhine, where several nuclear power plants are located. We extract daily temperature and
78 precipitation data over this domain from a large data set, comprising simulations of the past, present
79 and the future from different set-ups (coupled and uncoupled simulations, global and regional
80 simulations, single member or ensemble simulations), reanalyses, dynamically downscaled reanalyses,
81 and observations. A total of 55,000 simulation years are available (Rajczak et al., 2018, the data are
82 available from this website: <https://doi.pangaea.de/10.1594/PANGAEA.886881>). In this study we
83 focus on experiments with regional and global models. The following ensembles are used:

- 84 • CCC400: An ensemble of 30 AMIP-type global GCM simulations using ECHAM5.4 at T63
85 and covering the period 1600–2005
- 86 • the CMIP5 ensemble of 25 simulations (historical and RCP8.5) covering the period 1900–
87 2100
- 88 • initial condition ensemble of 21 COSMO simulations (0.44°) using the RCP8.5 scenario and
89 covering the years 1950–2100
- 90 • a set of 13 ENSEMBLES simulations using the A1B scenario and covering the period 1971–
91 2100
- 92 • a set of 15 CORDEX-11 simulations at 0.11° resolution (RCP8.5 and RCP4.5) covering the
93 period 1970–2099
- 94 • a set of 17 (RCP4.5) and 19 (RCP8.5) CORDEX-44 simulations at 0.44° resolution covering
95 the period 1970–2099

96 Table 1 gives an overview of all experiments used in our study, including references. The fact that the
97 data sets differ in several key aspects (e.g., resolution, time period covered, scenario used, complexity
98 of the model) allows a comprehensive view of possible changes and sources of uncertainties.

99 A consistent analysis of the available data sources is hardly feasible, as the data stems from models
100 with vastly different resolution and characteristics. All models suffer to some extent from biases. The
101 variety of modelling approaches thereby implies significant model-to-model differences. For this
102 reason, we focus on a fairly large catchment (where all models should arguably have at least some
103 potential), and use a statistical approach (quantile mapping) to calibrate the simulation results against
104 observations.

105 More specifically, the data are quantile-mapped (Themessl et al., 2011; Gudmundsson et al., 2012;
106 Teutschbein and Seibert, 2012; Rätty et al., 2014) to observation-based time series representative of the
107 average over the Aare catchment in Switzerland (see Fig. 1 for the stations; Fig. S1 shows the
108 observation-based, annual time series). Both data sets are used with daily resolution. The data and bias
109 correction are described in detail in Rajczak et al. (2018). The method has recently been used in other
110 Swiss climate impact studies (Rajczak et al., 2016a), and is reasonably skilful in daily and multi-day
111 precipitation diagnostics (Rajczak et al., 2016b). The transfer-function depends on the season and is
112 based on a 91-day moving window, centred over the day of the year (Themessl et al., 2012; Wilcke et
113 al., 2013; Rajczak et al., 2016a, 2016b). Values above the observed range of values are corrected
114 according to the 99.9th percentile (p99.9) in a constant manner (p1 and p99 in the case of temperature).
115 Studies recommend such an implementation opposed to complex extrapolation methods (Gutjahr and
116 Heinemann, 2013; Ivanov and Kotlarski, 2017; Themessl et al., 2012). Comparisons of raw and
117 quantile-mapped data are shown in Fig. S2. Note that quantile mapping does affect mean temperature
118 as well as temperature at the event day, which implies changes in saturation specific humidity. It is
119 therefore important to perform all analyses also for the raw data.

120 The analysis focuses on Rx1day, the maximum Rx1day per decade, annual mean temperature,
121 temperature at the event day, and the day of year of the event. All analyses are applied to each
122 individual simulation; only then the ensemble statistics are formed. No further weighting is performed
123 for multi-model data sets, but for some analyses the simulations are separated into those exhibiting a
124 drying or a wetting. We have performed all analyses for both the raw and quantile-mapped data. We
125 refer to the raw data occasionally in the text, more comprehensive material is added to the
126 supplementary material. For our analyses the following approach is used:

127 (i) We analyse long-term changes in Rx1day in each data set and compare this to the long-term
128 changes in annual mean temperature and as well as the trend in temperature at the event day. This
129 gives an indication of the proximity of trends in precipitation changes to a Clausius-Clapeyron scaling.

130 (ii) Changes in the seasonal cycle of temperature and event frequency (see below) are then addressed
131 by partitioning the data sets into sub-periods. For simulations of past climate (CCC400), we partition
132 the data from 1601–2000 into century chunks. For the present and future, for reasons of consistency,
133 we show results only for the two 35-yr periods 1971–2005 and 2065–2099, which are common to all
134 model experiments. In the supplementary material we also show results for all future simulations

135 partitioned into three periods of equal length (four periods for the longer simulations CMIP5 and
136 CCC400) to make full use of all data.

137 (iii) Within the periods, we analyse the seasonal cycle of the relative frequency of Rx1day events as
138 well as the seasonal cycle of temperature at the event day. The former indicates whether the
139 seasonality of Rx1day events changes, which is likely to affect the temperature trend on event days.
140 The latter takes this seasonality shift into account and indicates whether for a given calendar day,
141 temperature trends on event days differ from trends on all days. The annual cycle of temperature for
142 all days and for event days is estimated by fitting the first two harmonics of the seasonal cycle.

143 (iv) Finally, we address the dependence of Rx1day seasonality changes on background climate trends.
144 This is done for multi-model ensembles by stratifying the simulations within an ensemble according to
145 their linear trend (obtained with least-squares regression) in annual or summer mean precipitation over
146 the period 1971–2099. This allows addressing common signatures, *e.g.*, whether drying models tend to
147 show stronger changes in seasonality than wetting models.

148

149 **3. Results**

150 Before analyzing the statistics of Rx1day, a short description of typical Rx1day events at the
151 catchment scale are provided. Figure S2 shows meteorological fields from the CERA20C reanalysis
152 (Laloyaux et al. 2018) for the three strongest Rx1day events. The ten strongest events are listed in
153 Table 2, along with references. The typical catchment-scale Rx1day event is caused by the passage of
154 a cold front related to an elongated trough or cut-off low situation with destabilisation and pre-frontal
155 convective activity. Such situations are often associated with convergence and lifting of moist air,
156 originating from the Mediterranean region, north of the Alps in a ‘Vb’-type flow situation (see also
157 Stucki et al. 2012, Messmer et al. 2015, 2017). The event in 1978 is a typical example (Courvoisier,
158 1978; Stucki et al., 2017), but the situations in 1954 and 2007 as well as many of the events listed in
159 Table 2 were similar (Schmutz et al., 2008). Although models may not well reproduce the flow
160 deformation by the Alps as well as orographic enhancement of convection, they are assumed to
161 reproduce the synoptic scale processes such as frontal systems, moisture transport, and uplift.

162 Time series of Rx1day for the ensembles CCC400 (1600–2005), CMIP5 (historical and RCP8.5,
163 1900–2100), the COSMO initial condition ensemble (RCP8.5, 1950–2100), the ENSEMBLES
164 simulations (A1B, 1971–2100), CORDEX-11 (RCP8.5, 1970–2099) and CORDEX-44 (RCP8.5,
165 1970–2099) are shown in Fig. 2 (top). Over the past 400 years, no change in Rx1day is found (the
166 same is true for past millennium simulations (Lehner et al., 2015) or the Twentieth Century Reanalysis
167 20CRv2c (Compo et al., 2011) included in Rajczak et al. (submitted); not shown). A slight increase in
168 Rx1day over the past 50 years appears in CMIP5 (historical). Note, that there are also indications at
169 the continental to global scale that the majority of RCMs and GCMs tend to underestimate the

170 observed intensification in heavy rainfall (Fischer and Knutti, 2016; Borodina et al., 2017).
171 Simulations for the future show a clear increase in Rx1day of around 10-20% in the ensemble mean.
172 In the CMIP5 ensemble, the upper range of the ensemble shows a stronger increase than the mean.

173 Annual mean temperature (Fig.2, bottom, red line) shows a pronounced increase of 4-6 °C in the 21st
174 century. According to the Clausius-Clapeyron relation, this would correspond to a 30-50% increase in
175 precipitation extremes, which is not the case. However, if we consider only the temperature on the day
176 of the Rx1day precipitation events (Fig. 2, bottom, full blue line, note that this time series is
177 smoothed), we find a smaller temperature increase for most of the simulations. For the 21st century, the
178 temperature increase during Rx1day events amounts to only 3 °C (CMIP5) or even just 1 °C
179 (COMSO), but with considerable differences between experiments. Trends in Rx1day of 10-20% thus
180 approximately follow the Clausius-Clapeyron scaling. The same analyses for raw data gives very
181 similar results (shown in Fig. S2).

182 As already stated above, the Clausius-Clapeyron argument is expected to apply for the largest events,
183 but not for intermediate events, and may be not even for Rx1day events. Ban et al. (2015) analyzed
184 convection-resolving climate simulations at a resolution of 2 km, and calculated the scaling rates as a
185 function of all-day percentiles in the Alpine region for summer (see their Fig. 4e). In terms of
186 percentiles, our Rx1day event class would correspond to roughly the 99.7th percentile, and at this event
187 category the scaling estimate of Ban et al. (2015) amounts to about 1-3%/°C. This is roughly
188 consistent with the results in Fig.2 (when using mean temperature changes). Nevertheless, Ban et al.
189 (2015) found that increases in precipitation intensity would approximately asymptote towards the
190 Clausius-Clapeyron rate at very high percentiles.

191 The lower part of Fig. 2 also shows the same analysis for the temperature taken at the highest Rx1day
192 per decade (dashed lines). Note that sample size here is very small except for CCC400 and CMIP.
193 Interestingly, in CMIP5 temperatures during these events increase more strongly than for all Rx1day
194 events. The trend resembles that of the annual mean.

195 Two factors can contribute to the fact that the temperature increase on Rx1day events is smaller than
196 the increase in the annual mean: (1) a change in the occurrence frequency of Rx1day events towards a
197 colder season or (2) a different change of the temperature on Rx1day events even for unchanged
198 seasonality. We first analyse the latter. Considering the seasonal cycle of temperature during Rx1day
199 events (Fig. 3, top row), we find that in summer, Rx1day events in the present occur on days that are
200 slightly colder than average, while those few Rx1day events that occur during the cold season occur
201 with warmer than average conditions. This is evident in both observations (long black dashes) and
202 model simulations. In the future, Rx1day events tend to occur on days that are even cooler than
203 average, *i.e.*, the trend on Rx1day events (the difference between 2065–2099 and 1971–2005 is shown
204 on the right) is ca. 1 °C smaller than the trend on all days. This holds for all model ensembles, and the

205 difference has no obvious seasonal cycle. Thus, part of the trend difference between Rx1day and all
206 days is unrelated to the seasonality of Rx1day.

207 The day-of-occurrence of Rx1day (Fig. 3, second row) shows a broad summer peak in the
208 observations. Several of the model simulations simulate two peaks, one in early summer (June) and
209 one in early fall (September). Both in the past (CCC400) and in the future, there is a trend towards
210 fewer occurrences during June and July and more during the neighbouring months, *i.e.*, both the early
211 summer and the early fall peaks shift towards the cold season. This becomes particularly clear when
212 plotting the difference in relative frequency as a function of day of year between 2065–2099 and
213 1971–2005 (Fig. 3, middle right) for each experiments. The mid-summer events become rare; their
214 occurrence already decreased by 10% during the past 400 years and might further decrease by 30% in
215 the future. This shift in seasonality explains the remaining difference in temperature trends between
216 Rx1day event days and all days.

217 As we use the periods 1971–2005 and 2065–2099, Figure 3 (second row) is based on 100 (left) or 35
218 (middle) values per ensemble member and results were then smoothed with a Gaussian kernel with a
219 bandwidth of 15 days. In order to exploit the full data set, we also partitioned each data set into equal-
220 sized bins (Fig. S3) and found very similar results. Note, also, that the change in seasonality is not due
221 to the quantile mapping but appears also in the raw data (see Fig. S2).

222 However, the above results depend on the rarity of events. When analyzing rarer events, such as the
223 highest Rx1day events per decade (Fig. 3, bottom; note that samples are large enough only for
224 CCC400 and CMIP5, results for other experiments are shown in Fig. S3), we find a different result.
225 These events are even more concentrated to mid-summer than Rx1day in the present climate (the mid-
226 summer dip almost vanishes). In CCC400, their occurrence is high throughout the summer whereas in
227 CMIP5 these are mostly early fall events. Interestingly, there is no change in the frequency of
228 occurrence over time. Hence, only moderately extreme events (with a frequency of once per year) are
229 affected by a change in seasonality and not the more extreme events.

230 What causes this change in seasonality? Given the limited number of variables at our disposition
231 (temperature, precipitation), it is not possible to properly disentangle dynamical and thermodynamical
232 contributions. However, analyzing differences between the ensemble members gives important
233 indications. Within ENSEMBLES, CORDEX-11, CORDEX-44, and CMIP5 the contributing
234 ensemble members are grouped according to their trend in annual or summer mean precipitation (Fig.
235 4) and the analysis of the frequency of occurrence is repeated. Clear differences are found between
236 ensemble simulations, which show a drying and ensemble members with a positive trend in
237 precipitation in summer and in the annual mean (Fig. 4), particularly in CMIP5 and CORDEX-44, less
238 so in ENSEMBLES and CORDEX-11. The wetting ensemble members show hardly any change in
239 seasonality or even an increased frequency in summer, while the drying members show a decrease in

240 the frequency of occurrence of Rx1day events in mid-summer. The inter-model variability is large as
241 the samples get smaller, but the signature is robust across the entire data set (see Fig. S4).

242 Drying might also explain the changing seasonality in CCC400, as the ensemble mean shows
243 decreasing precipitation over the past 400 years (Fig. S6). Note that a mis-specified trend in land-
244 surface parameters might affect CCC400 (Rohrer et al., 2018). However, a simulation with corrected
245 land surface shows the same change in seasonality (Fig. S3).

246

247 **4. Discussion**

248 Heavy precipitation events (Rx1day) in the Aare catchment in the present climate are most frequent
249 during the warm season. If all preconditions (atmospheric circulation, stability, soil moisture, etc.) are
250 conducive to a heavy precipitation event, the intensity of the event is then expected to depend mainly
251 on thermodynamics, *i.e.*, on saturation specific humidity. It will thus follow a Clausius-Clapeyron
252 scaling as a first order approximation, often summarized as thermodynamic changes. In fact, trends in
253 Rx1day over the Aare catchment do follow a Clausius-Clapeyron scaling, however not of annual mean
254 temperature but rather of event-day temperature. This is because Rx1day may also change due to
255 dynamic changes *e.g.*, conducive conditions become less frequent and are not reached each summer.
256 Such changes may relate to changes in the large-scale circulation patterns or enhanced atmospheric
257 stability (*e.g.* Kröner et al., 2017) leading to reduced vertical updrafts (Pfahl et al., 2017).

258 In this respect, Rx1day and decadal-scale events exhibit a different behaviour in that the former show
259 a change in seasonality while the later do not. This discrepancy may be interpreted in the following
260 way: Decadal-scale precipitation extremes are mainly thermodynamically limited, *i.e.*, chances are
261 high that within a decade, conducive conditions occur on a late summer day, when temperatures and
262 thus saturation specific humidity are highest. In the future, such conditions can still be reached in late
263 summer once per decade, and thus the increase in temperature leads to an intensification of the most
264 extreme events, with no apparent change in seasonality, consistent with Ban et al. (2015). However, on
265 an annual scale such conditions are not reached every summer. Even in the present climate, Rx1day
266 events do not occur most frequently at the warmest time of the year. This indicates that other factors
267 (which we termed preconditions above) matter and Rx1day events are not fully thermodynamically
268 limited. This tendency will strengthen in the future as preconditions change, leading to a change in
269 seasonality. This result is consistent though more pronounced than identified by Pfahl et al. (2017)
270 who found a change of Rx1day events towards lower saturation specific humidity over the northern
271 extratropical land areas, indicating that the behaviour found in our analysis may be true for other
272 extratropical land regions as well.

273 While we cannot disentangle the contributions of individual factors to the preconditions, we can
274 identify drying as one of the important factors in models. Models that show a drying trend tend to

275 exhibit a shift in the seasonal cycle of moderate extremes (Rx1day) away from late-summer towards
276 early summer and fall, whereas the others do not.

277 A further result of our study is that even for a given calendar day, the future temperature trend in the
278 models is smaller for Rx1day than for all days. A possible explanation, particularly for summer days,
279 is model drying and thus excessive heating on non-precipitation days. In fact, stratifying the
280 simulations according to their summer-mean precipitation trends indicates that drying simulations
281 have a stronger cooling of event days relative to all days (Fig. S5).

282 The findings of our study - intensification of the most extreme events and change of seasonality for
283 moderate extremes - is relevant for adapting to future climatic changes. This is particularly the case as
284 observational coverage of the highest Rx1day per decade is limited. Whether or not the seasonality
285 shift is a real effect or occurs due to artificial summer drying of the models remains to be studied.
286 More detailed studies of the underlying processes, including stability and atmospheric circulation,
287 during future extreme events are also required (*e.g.*, Messmer et al. submitted).

288

289 **5. Conclusions**

290 Over the Alpine region moderate precipitation extremes such as characterized by Rx1day may not
291 increase as much as expected from applying a Clausius-Clapeyron to the change in annual mean
292 temperature, due to a change in seasonality of Rx1day events, and due to smaller-than-average
293 temperature trends during event days (regardless of the season). Both reasons are due to the fact that
294 moderate extreme events are not purely thermodynamically limited. In our study, we find that Rx1day
295 events in a future climate tend to occur less frequently in mid-summer, but more often in spring and
296 autumn. A similar change is also found over the past 400 years in model simulations. Further analyses
297 show that mostly those models are concerned whose annual mean or summer mean precipitation
298 decreases, *i.e.*, the changing seasonality is in part due to drying. Conversely, 10-yr events do exhibit
299 their highest frequency in mid-summer also in the future, with no apparent change in seasonality.

300 For flood protection this means that moderate events might shift towards the cold season with only a
301 small change in intensity, but the more relevant extreme events such as those with 10-yr return period
302 remain in summer and increase strongly in intensity.

303

304 **Acknowledgements.** This work was funded by the Swiss Federal Office for the Environment (FOEN),
305 the Swiss Federal Office of Energy (SFOE), and the Swiss Federal Nuclear Safety Inspectorate (ENSI)
306 in the framework the project EXAR: Understanding Extreme Flooding Events Aare-Rhein in
307 Switzerland as well as by the Swiss National Science Foundation (project 200021_143219 “EXTRA-
308 LARGE”). We acknowledge the World Climate Research Programme's Working Group on Regional

309 Climate, and the Working Group on Coupled Modelling, former coordinating body of CORDEX and
310 responsible panel for CMIP5. We also thank the climate modelling groups (listed in Table S1 of this
311 paper) for producing and making available their model output. We also acknowledge the Earth System
312 Grid Federation infrastructure an international effort led by the U.S. Department of Energy's Program
313 for Climate Model Diagnosis and Intercomparison, the European Network for Earth System Modelling
314 and other partners in the Global Organisation for Earth System Science Portals (GO-ESSP). Compute
315 facilities for the CCC400 simulations were provided by the Swiss National Supercomputing Centre
316 (CSCS). The Twentieth Century Reanalysis Project is supported by the U.S. Department of Energy
317 (DOE) Office of Science Innovative and Novel Computational Impact on Theory and Experiment
318 (INCITE) program, and Office of Biological and Environmental Research (BER), and by the National
319 Oceanic and Atmospheric Administration Climate Program Office

320

321 **References**

- 322 Allen, M. R., and Ingram, W. J.: Constraints on future changes in climate and the hydrologic cycle,
323 *Nature*, 419, 224–232, 2002.
- 324 Ban, N., Schmidli, J., and Schär, C.: Evaluation of the convection-resolving regional climate
325 modelling approach in decade-long simulations, *J. Geophys. Res. Atmos.*, 119, 7889–7907, doi:
326 10.1002/2014JD021478, 2014.
- 327 Ban, N., Schmidli, J., and Schär, C.: Heavy precipitation in a changing climate: Does short-term
328 summer precipitation increase faster? *Geophys. Res. Lett.*, 42, 1165–1172,
329 doi:10.1002/2014GL062588, 2015.
- 330 Begert, M.: Die Repräsentativität der Stationen im Swiss National Basic Climatological Network
331 (Swiss NBCN), *Arbeitsberichte der MeteoSchweiz* 217, 2008.
- 332 Bezzola, G. R. and Ruf, W. (Ed.): Ereignisanalyse Hochwasser August 2007. Analyse der Meteo- und
333 Abflussvorhersagen; vertiefte Analyse der Hochwasserregulierung der Jurarandgewässer. *Umwelt-*
334 *Wissen* Nr. 0927. Bundesamt für Umwelt, Bern, 209 pp, 2009.
- 335 Bhend, J., Franke, J., Folini, D., Wild, M., and Brönnimann, S.: An ensemble-based approach to
336 climate reconstructions, *Clim. Past*, 8, 963–976, doi:10.5194/cp-8-963-2012, 2012.
- 337 Borodina, A., Fischer, E. M., and Knutti, R.: Models are likely to underestimate increase in heavy
338 rainfall in the extratropical regions with high rainfall intensity, *Geophys. Res. Lett.*, 44, 7401–7409,
339 2017.
- 340 Compo, G. P., Whitaker, J. S., Sardeshmukh, P. D., Matsui, N., Allan, R. J., Yin, X., Gleason, B. E.,
341 Vose, R. S., Rutledge, G., Bessemoulin, P., Brönnimann, S., Brunet, M., Crouthamel, R. I., 1035
342 Grant, A. N., Groisman, P. Y., Jones, P. D., Kruk, M. C., Kruger, A. C., Marshall, G. J., Maugeri,

343 M., Mok, H. Y., Nordli, Ø., Ross, T. F., Trigo, R. M., Wang, X. L., Woodruff, S. D., and Worley,
344 S. J.: The Twentieth Century Reanalysis Project, *Q. J. Roy. Meteor. Soc.*, 137, 1–28, 2011.

345 Courvoisier, H. W., Gensler, G. A., Primault, B., and Roesli, H. P.: Das Unwetter vom 7./8. August
346 1978 in der Schweiz. Arbeitsberichte der Schweizerischen Meteorologischen Zentralanstalt Nr. 85,
347 1979.

348 Fischer, E. M., and Knutti, R.: Anthropogenic contribution to global occurrence of heavy-precipitation
349 and high-temperature extremes, *Nature Climate Change*, 5, 560–564, 2015.

350 Fischer, E. M., and Knutti, R.: Observed heavy precipitation increase confirms theory and early
351 models, *Nature Climate Change*, 6, 986–991, 2016.

352 Giorgi, F., Torma, C., Coppola, E., Ban, N., Schär, C., and Somot, S.: Enhanced summer convective
353 rainfall at Alpine high elevations in response to climate warming, *Nature Geoscience* 9, 584–589,
354 2016.

355 Gudmundsson, L., Bremnes, J. B., Haugen, J. E., and Engen-Skaugen, T.: Technical Note:
356 Downscaling RCM precipitation to the station scale using statistical transformations - a comparison
357 of methods, *Hydrol. Earth Syst. Sci.*, 16, 3383–3390, 2012.

358 Gutjahr O., and Heinemann, G.: Comparing precipitation bias correction methods for high-resolution
359 regional climate simulations using COSMO-CLM, *Theor. Appl. Climatol.*, 114, 511–529, doi:
360 10.1007/s00704-013-0834-z, 2013.

361 Ivanov. M. and Kotlarski, S.: Assessing distribution-based climate model bias correction methods over
362 an alpine domain: added value and limitations, *Int. J. Climatol.*, 37, 2633–2653, doi:
363 10.1002/joc.4870, 2016.

364 Jacob, D., et al.: EURO-CORDEX: new high-resolution climate change projections for European
365 impact research, *Regional Environmental Change*, 14, 563–578, 2014.

366 Kotlarski, S., Keuler, K., Christensen, O. B., Colette, A., Déqué, M., Gobiet, A., Goergen, K., Jacob,
367 D., Lüthi, D., van Meijgaard, E., Nikulin, G., Schär, C., Teichmann, C., Vautard, R., Warrach-Sagi,
368 K., and Wulfmeyer, V.: Regional climate modeling on European scales: a joint standard evaluation
369 of the EURO-CORDEX RCM ensemble, *Geosci. Model Dev.*, 7, 1297–1333,
370 <https://doi.org/10.5194/gmd-7-1297-2014>, 2014.

371 Kröner, N., Kotlarski, S., Fischer, E., Lüthi, D., Zubler, E., and Schär, C.: Separating climate change
372 signals into thermodynamic, lapse-rate and circulation effects: theory and application to the
373 European summer climate, *Clim. Dyn.* 48, 3425–3440, 2017

374 Laloyaux, P., de Boisseson, E., Balmaseda, M., Bidlot, J.-R., Brönnimann, S., Buizza, R., Dalhgren,
375 P., Dee, D., Haimberger, L., Hersbach, H., Kosaka, Y., Martin, M., Poli, P., Rayner, N.,
376 Rustemeier, E., and Schepers, D.: CERA - 20C: A coupled reanalysis of the Twentieth Century. *J.*
377 *Adv. Model. Earth Syst.*, doi:10.1029/2018MS001273, 2018

378 Lehner, F., Keller, K., Raible, C. C., Mignot, J., Born, A., Joos, F., and Stocker, T. F.: Climate and
379 carbon cycle dynamics in a CESM simulation from 850 - 2100CE, *Earth System Dynamics*, 6,
380 411 - 434, 2015.

381 Messmer, M., Gomez-Navarro, J. J., and Raible, C. C.: Climatology of Vb-cyclones, physical
382 mechanisms and their impact on extreme precipitation over Central Europe, *Earth System*
383 *Dynamics*, 6, 541–553, 2015.

384 Messmer, M., Gomez-Navarro, J. J. and Raible, C. C.: The Impact of Vb-Cyclones to Ocean
385 Temperature and Soil Moisture Changes in Sensitivity Experiments with WRF. *Earth System*
386 *Dynamics*, 8, 477–493, 2017.

387 Messmer, M., Gomez-Navarro, J. J., and Raible, C. C.: The Impact of Climate Change on the
388 Climatology of Vb-Cyclones, *Tellus*, submitted, 2018.

389 MeteoSchweiz, Starkniederschlagsereignis August 2005, *Arbeitsberichte der MeteoSchweiz*, 211, 63
390 pp., 2006.

391 Pendergrass, A. G.: What precipitation is extreme? *Science* 360, 1072-1073, 2018.

392 Pfahl S.: Characterising the relationship between weather extremes in Europe and synoptic circulation
393 features, *Nat. Hazards Earth Syst. Sci.* 14, 1461–1475, 2014.

394 Pfahl, S., O’Gormann, P. A., and Fischer, E. M.: Understanding the regional pattern of projected
395 future changes in extreme precipitation, *Nature Geoscience*, 7, 423–427, 2017.

396 Prein, A. F., Langhans, W., Fosser, G., Ferrone, A., Ban, N., Goergen, K., Keller, M., Tölle, M.,
397 Gutjahr, O., Feser, F., Brisson, E., Kollet, S., Schmidli, J., van Lipzig, N. P. M., and Leung, R.: A
398 review on regional convection-permitting climate modeling: Demonstrations, prospects, and
399 challenges, *Rev. Geophys.*, 53, 323–361, doi:10.1002/2014RG000475, 2015.

400 Rajczak J., Kotlarski S., and Schär, C.: Does quantile mapping of simulated precipitation correct for
401 biases in transition probabilities? *J. Clim.*, 29, 1605–1615, doi: 10.1175/JCLI-D-15-0162.1, 2016a.

402 Rajczak J., Kotlarski, S., Salzmänn N., and Schär, C.: Robust climate scenarios for sites with sparse
403 observations: A two-step bias correction approach, *Int. J. Climatol.*, 36, 1226–1243. doi:
404 10.1002/joc.4417, 2016b.

405 Rajczak, J., Brönniman, S., Fischer, E. M., Raible, C. C., Rohrer, M., Sørland, S. L., and Schär, C.:
406 Daily precipitation and temperature series from multiple climate model simulations for the Aare
407 river catchment in Switzerland, in submission.

408 Rätty, O., Räisänen, J., and Ylhäisi, J.: Evaluation of delta change and bias correction methods for
409 future daily precipitation: intermodel cross-validation using ENSEMBLES simulations, *Climate*
410 *Dynamics* 42, 2287–2303, doi:10.1007/s00382-014-2130-8, 2014.

411 Rohrer, M., Brönnimann, S., Martius, O., Raible, C. C., Wild, M., and Compo, C. P.: Representation
412 of extratropical cyclones, blocking anticyclones, and Alpine circulation types in multiple
413 reanalyses and model simulations, *J. Clim.* 31, 3001–3031, 2018, doi:10.1175/JCLI-D-17-0350.1.

414 Schär, C., Ban, N., Fischer, E. M., Rajczak, J., Schmidli, J., Frei, C., Giorgi, F., Karl, T. R., Kendon,
415 E. J., Klein Tank, A. M. G., O’Gorman, P. A., Sillmann, J., Zhang, X., Zwiers, F. W.: Percentile
416 indices for assessing changes in heavy precipitation events, *Climatic Change*, 137, 201–216,
417 <http://dx.doi.org/10.1007/s10584-016-1669-2>, 2016.

418 Scherrer, S. C., Fischer, E. M., Posselt, R., Liniger, M. A., Croci-Maspoli, M., and Knutti, R.:
419 Emerging trends in heavy precipitation and hot temperature extremes in Switzerland, *J. Geophys.*
420 *Res. Atmos.*, 121, doi:10.1002/2015JD024634, 2016.

421 Schmutz, C., Arpagaus, M., Clementi, L., Frei, C., Fukutome, S., Germann, U., Liniger, M., and
422 Schacher, F.: Meteorologische Ereignisanalyse des Hochwassers 8. bis 9. August 2007,
423 *Arbeitsberichte der MeteoSchweiz*, 222, 30 pp., 2008.

424 Stucki, P., Rickli, R., Brönnimann, S., Martius, O., Wanner, H., Grebner, D., and Luterbacher, J.: Five
425 weather patterns and specific precursors characterize extreme floods in Switzerland, *Meteorol. Z.*,
426 21, 531–550, 2012.

427 Stucki, P., Baumann, A., and Bucher, D.: The 1978 Heavy Precipitation and Flood Event in
428 Switzerland. In: Brönnimann, S. (Ed.) *Historical Weather Extremes in Reanalyses*. *Geographica*
429 *Bernensia G92*, p. 69–80, DOI: 10.4480/GB2017.G92.06, 2017.

430 Taylor, K. E., Stouffer, R. J., and Meehl, G. A.: An Overview of CMIP5 and the Experiment Design,
431 *B. Am. Meteorol. Soc.*, 93, 485–498. doi:10.1175/BAMS-D-11-00094.1, 2012.

432 Teutschbein, C., and Seibert, J.: Bias correction of regional climate model simulations for hydrological
433 climate-change impact studies: Review and evaluation of different methods, *Journal of Hydrology*,
434 456–457, 12-29, 2012.

435 Themessl, M., Gobiet, A., and Leuprecht, A.: Empirical-statistical downscaling and error correction of
436 daily precipitation from regional climate models, *Int. J. Climatol.*, 31, 1530–1544, 2011.

437 Themessl, M., Gobiet, A., and Leuprecht, A.: Empirical-statistical downscaling and error correction of
438 regional climate models and its impact on the climate change signal, *Climatic Change*, 112, 449–
439 486, doi: 10.1007/s10584-011-0224-4, 2012.

440 Van Bebber, W.: Die Zugstrassen der barometrischen Minima nach den Bahnenkarten der deutschen
441 Seewarte für den Zeitraum 1875–1890, *Meteorol. Z.*, 8, 361–366, 1891.

442 Van der Linden, P. and Mitchell, J. F. B.: *ENSEMBLES: Climate change and its impacts: Summary of*
443 *research and results from the ENSEMBLES Project*, MetOffice Hadley Centre, Exeter, UK, 2009.

444 Van Vuuren, D. P., Edmonds, J., Kainuma, M., Riahi, K., Thomson, A., Hibbard, K., Hurtt, G. C.,
445 Kram, T., Krey, V., Lamarque, J.-F., Masui, T., Meinshausen, M., Nakicenovic, N., Smith, S. J.,

- 446 Rose, S. K.: The representative concentration pathways: an overview, *Climatic Change*, 109, 5–31,
447 doi:10.1007/s10584-011-0148-z, 2011.
- 448 Wilcke, R. A. I., Mendlik, T., and Gobiet, A.: Multi-variable error correction of regional climate
449 models, *Climatic Change*, 120, 871–887, doi: 10.1007/s10584-013-0845-x, 2013.
- 450 Zhang, X., Zwiers, F. W., Li, G., Wan, H, and Cannon, A. J.: Complexity in estimating past and future
451 extreme short-duration rainfall, *Nature Geoscience* 10, 255–259, 2017.

452 **Tables**

453 **Table 1.** Overview of model experiments used in our study (see Table S1 for further details)

Experiment	Type	Resol.	<i>n</i>	Period	Scenario	Reference
CCC400	Global GCM	2°	30+1*	1600–2005	Historical	Bhend et al. (2012) Rohrer et al. (2018)
CMIP5	Global AOGCM	various	25	1901–2100	Historical, RCP8.5	Taylor et al. (2012)
ENSEMBLES	Regional	25 km	13	1970–2099	A1B	van der Linden and Mitchell (2009)
COSMO	Regional	0.44°	21	1950–2100	RCP8.5	
CORDEX-11	Regional	0.11°	15	1971–2099	RCP8.5	
CORDEX-44	Regional	0.44°	19	1971–2099	RCP8.5	
CORDEX-11	Regional	0.11°	15	1971–2099	RCP4.5	Jacob et al. (2014); Kotlarski et al. (2014)
CORDEX-44	Regional	0.44°	17	1971–2099	RCP4.5	

454 * Trends in some land-surface properties were mis-specified in the 30-member ensemble, an additional member with
 455 corrected land-surface properties was performed to assess the errors (Rohrer et al., 2018). The figures in this paper show the
 456 30 member ensemble; results for the land-surface corrected member share the same features and are shown in Fig. S3.

457

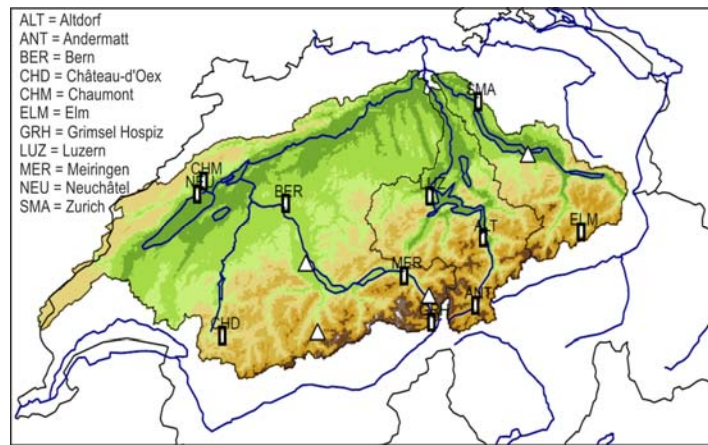
458 **Table 2.** The largest ten Rx1day events in the catchment-averaged observations sorted by their
 459 strength.

Year	Mon	Day	Rx1day (mm)	Comment
1978	8	7	84.8	62% of Swiss area >70 mm/d (Courvoisier et al. 1979), flooding of Rhine (Stucki et al. 2017), max Rx1day at several stations in the region (MeteoSwiss, 2006)
1954	8	21	76.5	39% of Swiss area >70 mm/d (Courvoisier et al. 1979)
2007	8	8	64.0	large flooding (Bezzola and Ruf, 2009), highest runoff at Aare (Untersiggental)
1908	5	23	55.0	max Rx1day at several stations in the region (MeteoSwiss, 2006)
1939	8	5	54.9	max Rx1day at one station in the region (MeteoSwiss, 2006)
2009	7	17	54.2	large damages due to (prefrontal) thunderstorms
1977	7	31	53.9	max Rx1day at one station in the region (MeteoSwiss, 2006)
1991	12	21	53.5	max Rx1day at several stations in the region (MeteoSwiss, 2006)
2005	8	21	53.1	major flood event in Switzerland (MeteoSwiss, 2006)
1910	6	14	52.4	major flood event in Switzerland (Stucki et al. 2012), 25% of Swiss area >70 mm/d (Courvoisier et al. 1979), max Rx1day at several stations in the region (MeteoSwiss, 2006)

460

461 **Figures**

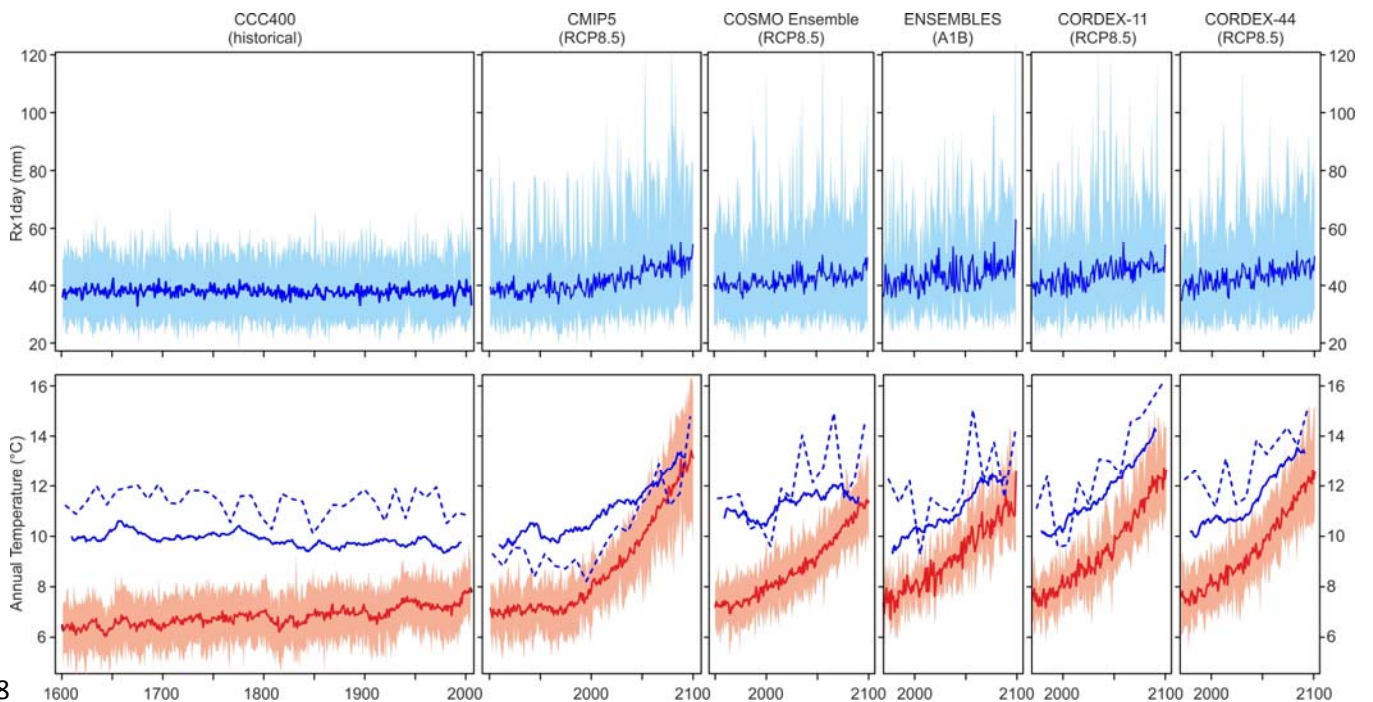
462



463

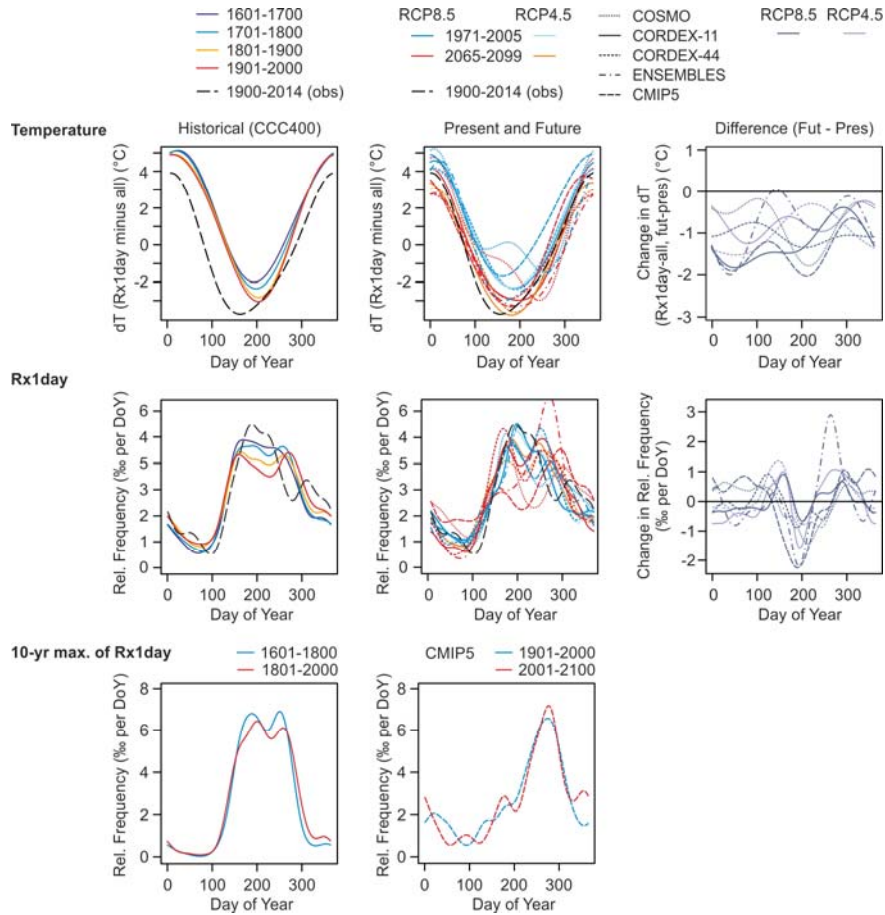
464 **Fig. 1:** Catchment of the Aare river. All data used in this study represent averages over this region.
 465 The representative weather stations are shown as squares (providing both temperature and
 466 precipitation) and triangles (only precipitation).

467



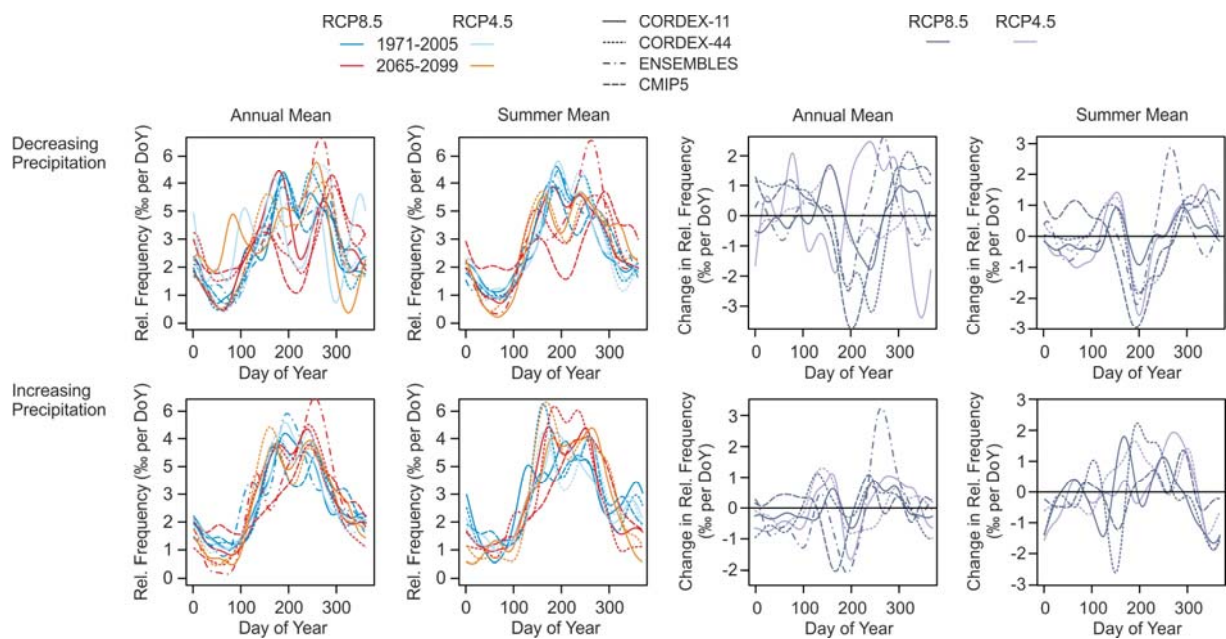
468

469 **Fig. 2:** Annual time series (ensemble mean as line and ensemble range as shading) of (top) Rx1day
 470 and (bottom) annual mean temperature (red) as well as the temperature during the Rx1day event (blue
 471 solid line, smoothed with a 20-yr running average) in CCC400, CMIP5 and COSMO (quantile
 472 mapped). Also shown is the temperature at the highest Rx1day event per decade (blue dashed;
 473 ensemble mean).



474

475 **Fig. 3:** (top row) Temperature difference as a function of calendar day between event days (Rx1day)
 476 and all days for different time periods in CCC400 (left) and in model simulations of the present
 477 (1971–2005) and future (2065–2099) (middle; the right figure shows the difference between the two
 478 periods). (middle row) Density plot of the day of occurrence of Rx1day events for different time
 479 periods in CCC400 (left) and in model simulations of the present (1971–2005) and future (2065–2099)
 480 (middle; the right figure shows the difference between the two periods). (bottom row) Same as second
 481 row, but only for the highest Rx1day per decade. Note that only CCC400 and CMIP5 have sufficiently
 482 large ensembles, and longer time periods were chosen. All analyses are based on quantile-mapped data
 483 (see Fig. S3 for additional plots and Fig. S2 for the same analysis based on raw data). A Gaussian
 484 Kernel smoother with a bandwidth of 15 days was used for plotting. Results from catchment-averaged
 485 observations are shown as long black dashes.



486

487 **Fig. 4:** Density plot of the day of occurrence of Rx1day for the present (1971–2005) and future (2065–
 488 2099) in different the multi-model ensembles (left two columns). The right two columns show the
 489 difference between future and present climate. Ensemble members are separated into those that show a
 490 positive or negative trend in annual mean (first and third column) or summer mean (second and fourth
 491 column) precipitation over the 1971–2099 period (see Fig. S4 for additional plots from other scenarios
 492 and different time periods).